PROGRESS IN PHOTOVOLTAICS: RESEARCH AND APPLICATIONS
Prog. Photovolt. Res. Appl. 2007; **15**:415–423
Published online 22 February 2007 in Wiley InterScience (www.interscience.wiley.com) DOI: 10.1002/pip.754

Research

Light Trapping Effect of Submicron Surface Textures in Crystalline Si Solar Cells

Hitoshi Sai[1]*,†, Yoshiaki Kanamori[2], Koji Arafune[1], Yoshio Ohshita[1] and Masafumi Yamaguchi[1]
[1]*Toyota Technological Institute, 2-12-1 Hisakata, Tempaku-ku, Nagoya 468-8511, Japan*
[2]*Graduate School of Engineering, Tohoku University, 6-6-01 Aoba, Aramaki Aoba-ku, Sendai 980-8579, Japan*

Recently, submicron textures have been researched and applied to multicrystalline silicon solar cells in order to improve their optical performance. In this study, the antireflection and light trapping effects of submicron surface textures in crystalline Si (c-Si) solar cells were quantitatively investigated by numerical simulations based on Maxwell's equations with a simple two-dimensional (2D) surface grating model. The calculated results showed that the surface reflection loss can be effectively reduced by using submicron Si surface gratings with appropriate aspect ratios. On the other hand, higher order diffractions that are caused by surface gratings that increase optical path lengths and light absorption near the band gap wavelength are dominant only for those with periods greater than 0·5 μm. From these results, it was inferred that submicron textures are effective for light trapping as well as for antireflection in thin c-Si solar cells if appropriate dimensions are chosen. Copyright © 2007 John Wiley & Sons, Ltd.

KEY WORDS: light trapping; surface texturing; submicron texture; antireflection; crystalline Si; diffraction

Received 15 December 2006; Revised 18 January 2007

INTRODUCTION

The global production of crystalline Si (c-Si) solar cells has been growing rapidly for the past 10 years; however, a further reduction in cost by using thinner Si substrates (∼50 μm) is required since the substrate cost comprises approximately half the cell module cost. Light trapping is more important in developing high-efficiency c-Si solar cells with thinner substrates because the absorption coefficient is substantially small near the bandgap wavelength (e.g., $\sim 100\,cm^{-1}$ at 1·0 μm). In general, surface texturing is widely used as a light confinement technique. By developing the surface structure on a Si substrate, the following three effects can be observed: (a) reduction in surface reflection, (b) increase in light absorption due to an increase in optical path length by diffraction, and (c) enhancement of internal reflection that reduces the amount of escaping light. Effect (a) is essential for increasing the input energy to solar cells, irrespective of the cell thickness. For thin Si substrates, effects (b) and (c) are vital for increasing light absorption at higher wavelengths.

* Correspondence to: Hitoshi Sai, National Institute for Advanced Industrial Science and Technology, Central 2, Umezono 1-1-1, Tsukuba 305-8568, Japan.
E-mails: hitoshi-sai@aist.go.jp; sai_hitoshi@yahoo.co.jp

Single c-Si solar cells are generally textured with random pyramids, which are produced by anisotropic wet chemical etching solutions such as those of KOH and NaOH.[1] In most of the cases, the random pyramids have dimensions in the range of several microns. The random nature of multicrystalline Si (mc-Si) makes such techniques considerably less effective for this material. For the past 10 years, surface texturing by dry processes such as reactive ion etching (RIE) has been investigated and applied to mc-Si solar cells.[2–5] By this technique, it is possible to uniformly produce very fine structures in the submicron range on a Si surface; moreover, the surface reflectivity can be reduced effectively. However, few studies have systematically and quantitatively investigated the light trapping effect of such submicron structures. The main reason is the difficulty in the optical analysis of such small structures. The optical properties of submicron textures in the visible and near infrared wavelengths cannot be quantitatively evaluated by a simple analysis based on the scalar theory such as the ray-tracing technique, in which the wavelengths of light are assumed to be sufficiently smaller than the typical dimensions of objects.[1,6,7] Therefore, more rigorous approaches are required. Thus, Abouelsaood *et al*.[8] have rigorously analyzed the light trapping effect of submicron Si gratings based on coupled-wave analysis. On the other hand, Heine and Morf[9] have measured the light trapping effect caused by well-defined submicron Si gratings on the rear side of c-Si solar cells. However, they have considered only one-dimensional gratings; therefore, further investigations are required.

In this study, the optical properties of submicron structures were evaluated with the help of numerical simulations. The diffraction (refraction) and surface reflection due to submicron surface structures were investigated from the viewpoint of light trapping in c-Si solar cells.

SIMULATION METHOD

We conducted numerical calculations on the basis of a rigorous coupled-wave analysis (RCWA),[10] which is a method that can be used to directly solve the Maxwell's electromagnetic equations. In a previous paper, we showed that the simulated results obtained by RCWA agree well with the experimental data, and that RCWA is an effective tool for estimating the optical behavior of submicron textures.[11]

For simplicity, the submicron textures investigated in this study were modeled by two-dimensional (2D) surface gratings composed of small pyramids without antireflective coatings. The pyramid grating region was symmetrical along the x and y directions and was approximated by a stack of 8 or 16 layers of Si slabs, as shown in Figure 1. The calculation parameters were the period Λ, grating depth d, and substrate thickness w. For some cases, an Al back surface reflector (BSR) was applied to the smooth rear surface. In all the calculations, the diffraction efficiencies, DE_{mn}, up to $\pm$7th were taken into account, where m and n are the diffraction orders for the x and y directions, respectively. In order to reduce the calculation time, plane waves with a fixed polarization angle of 45° were used as the incident light instead of a randomly polarized light. This is a good assumption of randomly polarized sunlight because the optical properties of 2D symmetrical gratings are essentially not

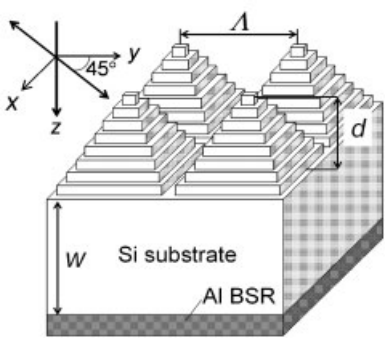

Figure 1. The Si cell model with submicron surface textures used for calculations in this study. Λ: period, d: grating depth, w: substrate thickness. For calculating surface reflection, the Si substrate was assumed to have infinite thickness

DOI: 10.1002/pip

sensitive to the polarization angle of the incident light. The optical constants of Si and Al were obtained from the literature.[12,13]

RESULTS AND DISCUSSION

Surface reflection

First, the surface reflectivity of the submicron textures was calculated by assuming that the Si substrate was infinitely thick. The surface reflectivity is of prime importance for increasing the photovoltaic energy conversion efficiencies because it determines the amount of light that enters into the cells and forms electron-hole pairs. Figure 2 shows the calculated spectral reflectivity of the 2D Si gratings at normal incidence for several different values of Λ under a constant aspect ratio, $d/\Lambda = 1{\cdot}0$. The reflectivity is decreased by developing the submicron textures over a wide range of wavelengths. This figure also shows that the reflectivity can be substantially decreased by increasing Λ from 0·1 μm to 0·4 μm for a constant value of d/Λ. Figure 3 shows the reflectivity spectra for several different values of d under a constant period, $\Lambda = 0{\cdot}2$ μm. The reflectivity can also be reduced by increasing d over a wide range of wavelengths, as shown in the figure. Figure 3 indicates that a very low reflectivity of less than 2% can be obtained by fabricating the surface gratings with a high aspect ratio, that is, $d/\Lambda > 2{\cdot}0$, for this case.

We calculated the surface reflectivity spectra of the submicron Si gratings for various values of Λ and d and determined the weighted reflectivity for the standard solar spectrum by the following equation:

$$R_{\text{solar}} = \frac{\int_{0{\cdot}3\,\mu\text{m}}^{1{\cdot}12\,\mu\text{m}} R(\lambda) N_{\text{photon}}(\lambda) d\lambda}{\int_{0{\cdot}3\,\mu\text{m}}^{1{\cdot}12\,\mu\text{m}} N_{\text{photon}}(\lambda) d\lambda} \tag{1}$$

where $R(\lambda)$ is the spectral reflectivity of the textured surfaces and N_{photon} is the photon number of the solar irradiation (AM1·5G) per unit area per unit wavelength. The bandgap wavelength of c-Si was set to 1·12 μm. The results shown in Figure 4 indicate that a low value of R_{solar} of less than 3% can be obtained by using a variety of submicron surface gratings. For $\Lambda > 0{\cdot}4$ μm, a low value of R_{solar} can be obtained with a reasonable value of

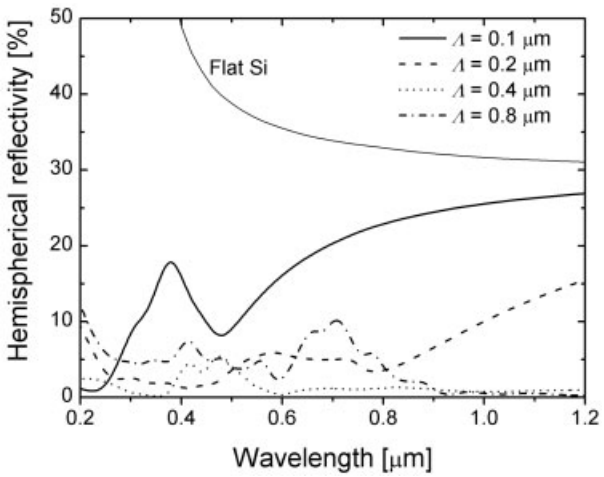

Figure 2. Calculated spectral reflectivity of submicron Si surface gratings for several values of Λ under a constant aspect ratio, $d/\Lambda = 1{\cdot}0$, at normal incidence

DOI: 10.1002/pip

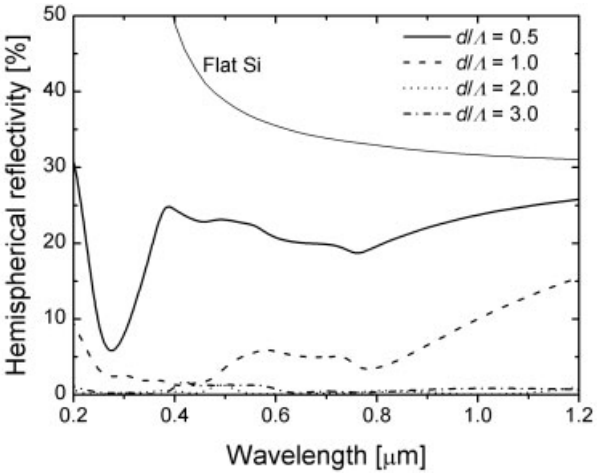

Figure 3. Calculated spectral reflectivity of submicron Si surface gratings with $\Lambda = 0{\cdot}2\,\mu m$ for several values of d/Λ at normal incidence

d/Λ (around unity). On the other hand, for small values of Λ of less than $0{\cdot}2\,\mu m$, a much larger value of d/Λ is required to reduce the surface reflection loss at the same level. A larger aspect ratio naturally results in a larger surface area, which enhances the surface recombination in solar cells. From these results, it is inferred that a submicron texture with $\Lambda > 0{\cdot}4\,\mu m$ is effective for reducing the surface reflection loss without severe surface recombination loss.

Forward diffraction

Once light enters into a solar cell with a surface grating, it propagates through the solar cell at a particular diffraction angle based on the diffraction order, schematically shown in Figure 5. The forward diffraction angle

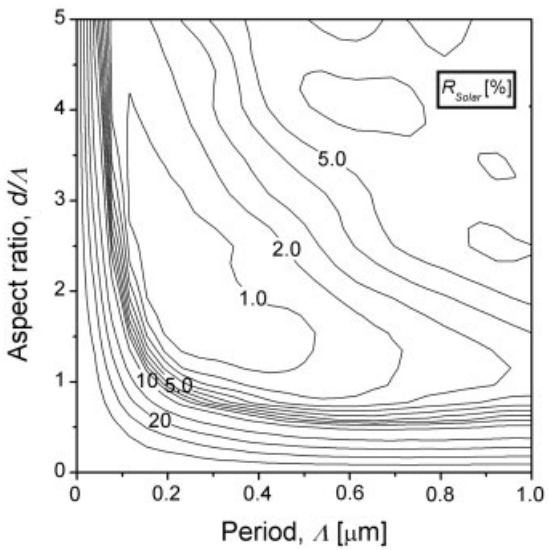

Figure 4. Contour map of the weighted reflectivity of submicron Si gratings as functions of Λ and d/Λ for the standard solar spectrum (AM1·5)

DOI: 10.1002/pip

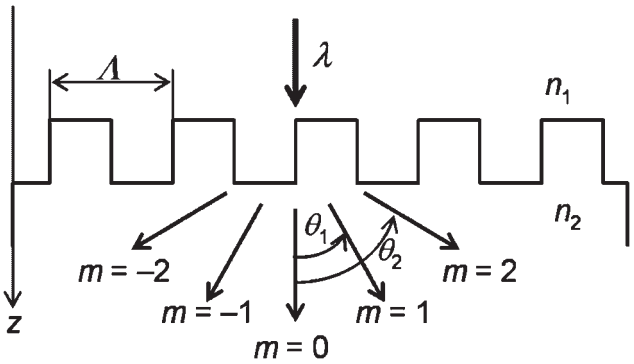

Figure 5. Schematic drawing of forward diffraction by 1D surface grating

θ_m of a one-dimensional surface grating is given by the following equation:[14]

$$n_2 \sin\theta_m = n_1 \sin\theta_i + m\frac{\lambda}{\Lambda} \tag{2}$$

where n_1 and n_2 are the refractive indices of mediums 1 and 2, respectively. Further, θ_i, the incident angle; θ_m, the diffraction angle at the diffraction order m ($m = 0, \pm 1, \ldots$); and λ, the wavelength. A similar expression is obtained for the backward diffraction, namely, reflection.

In the case of 2D Si gratings, the diffraction angles for normal incidence are given by:

$$n_{Si} \sin\theta_{mn} \cos\phi_{mn} = m\frac{\lambda}{\Lambda_x} \tag{3-1}$$

$$n_{Si} \sin\theta_{mn} \sin\phi_{mn} = n\frac{\lambda}{\Lambda_y} \tag{3-2}$$

where θ_{mn} and ϕ_{mn} are the diffraction polar angle and the azimuthal angle at the diffraction order of (m, n), respectively. Note that the diffraction angles are basically independent of the grating depth, d.

Figure 6 shows the values of θ_{mn} of symmetrical 2D gratings ($\Lambda = \Lambda_x = \Lambda_y$) as functions of normalized wavelengths, λ/Λ, for several sets of diffraction orders. In this figure, a constant refractive index ($n_{Si} = 3{\cdot}6$) was considered. Figure 6 reveals that no high order diffractions occur in the case of $\lambda/\Lambda > 4$. For such structures, the entire incident light propagates through the medium in a straight direction. This is a typical behavior of

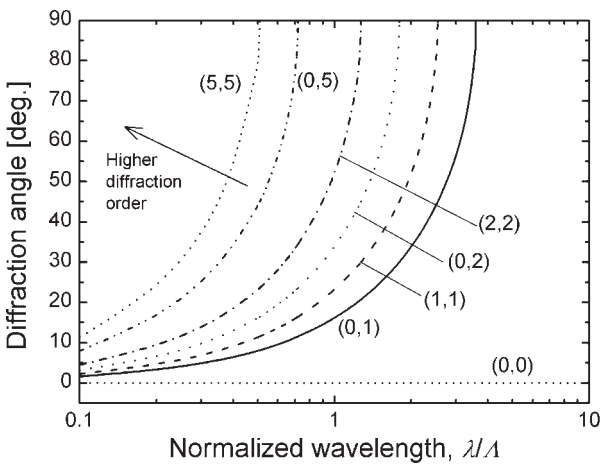

Figure 6. Diffraction angles θ_{mn} as functions of normalized wavelength, λ/Λ at several diffraction orders (m, n) for 2D symmetrical Si grating ($n_{Si} = 3{\cdot}6$)

DOI: 10.1002/pip

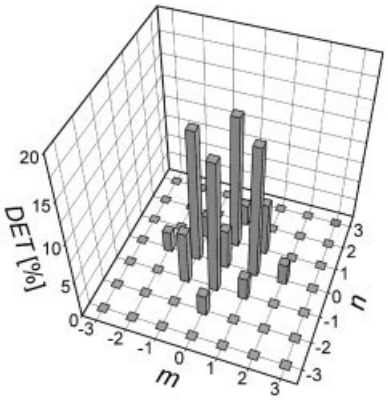

Figure 7. Distribution of the forward diffraction efficiencies DET_{mn} of 2D Si pyramid grating with $\Lambda = 0{\cdot}6\,\mu m$ and $d/\Lambda = 1{\cdot}0$ at $\lambda = 1{\cdot}0\,\mu m$

subwavelength structures whose Λ is much lesser than λ ($\lambda/\Lambda >> 1$). This result shows that very small structures are not effective for increasing the optical path lengths by diffraction.

The next question is how the transmitted light is distributed between each diffraction order, in other words, each diffraction angle. The forward (transmission) diffraction efficiencies for each diffraction order (m, n), DET_{mn}, can be obtained by RCWA calculations. Figure 7 shows the calculated DET distribution for the 2D Si pyramid grating with $\Lambda = 0{\cdot}6\,\mu m$ and $d/\Lambda = 1{\cdot}0$ at $\Lambda = 1{\cdot}0\,\mu m$. In this case, most of the transmitted light is distributed between the $(0, \pm 1)$ and $(\pm 1, 0)$ orders and the DET_{00} value is only 5%. The light distributed among the higher orders, particularly, $(m, n) \neq (0, 0)$, propagates through Si at oblique angles. Consequently, there is an increase in the light absorption in the c-Si solar cells with finite thicknesses, particularly for longer wavelengths at which the absorption coefficient of c-Si is small.

Here, we define DET for higher orders, DET_{HO}, which quantifies the contribution to light trapping as follows:

$$DET_{HO} = \sum_{m=-\infty}^{\infty} \sum_{n=-\infty}^{\infty} DET_{mn} - DET_{00} \tag{4}$$

DET_{HO} is the summation of DET_{mn} for all DET values except DET_{00}. In this study, the summation was performed in the range from -7 to $+7$. In Figure 8, DET_{HO} is plotted as a function of wavelength for several Si pyramid gratings with $d/\Lambda = 1{\cdot}0$. The absorption length (reciprocal of absorption coefficient) of c-Si is also plotted for comparison. For increasing values of Λ, DET_{HO} increases up to approximately 100% for

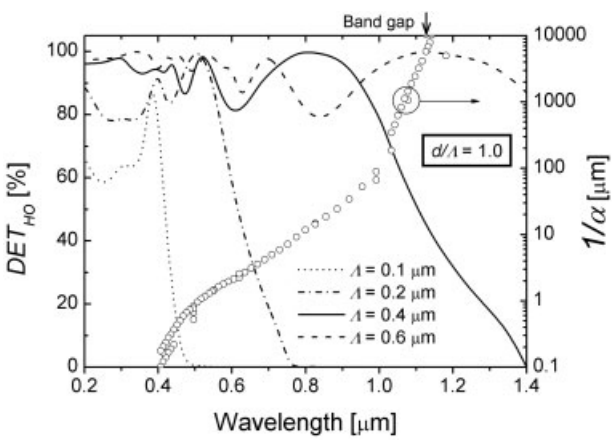

Figure 8. Higher order DET of 2D Si pyramid gratings with $d/\Lambda = 1{\cdot}0$ as a function of wavelength for several different values of Λ. The circular symbols show the absorption length of c-Si[12]

DOI: 10.1002/pip

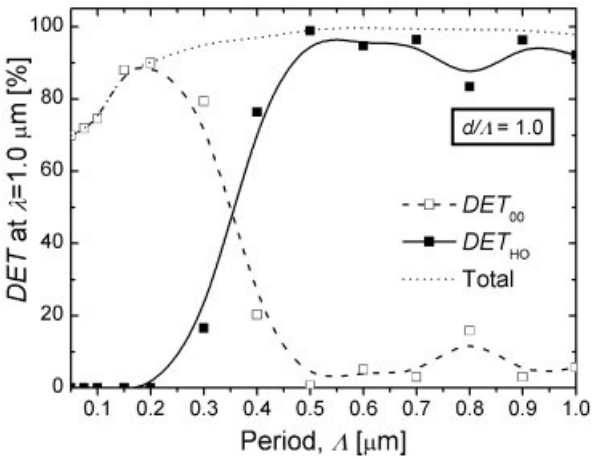

Figure 9. DET of 2D Si pyramid gratings with $d/\Lambda = 1{\cdot}0$ as a function of Λ at $\lambda = 1{\cdot}0\,\mu m$

longer wavelengths at which the absorption coefficient of c-Si is small. This contributes to effective light trapping in c-Si solar cells made of thin substrates.

In Figure 9, DET is plotted as a function of Λ at a constant wavelength, $\lambda = 1{\cdot}0\,\mu m$. The behavior of DET can be categorized into three regions: the region where only DET_{00} is generated (region 1), the region where DET_{HO} is dominant (region 2), and the transient region (region 3). Clearly, region 2 is preferable from the viewpoint of light trapping. From Figure 9, it is inferred that surface textures larger than $0{\cdot}5\,\mu m$ are suitable for achieving effective light trapping in thin c-Si cells as well as for achieving low surface reflectivity.

Cell structure

In the previous two sections, the surface reflection and the diffraction of the submicron Si gratings were discussed for a Si substrate that was assumed to have infinite thickness. In the following section, we consider a Si cell model with a finite substrate thickness w and a rear Al-BSR, as shown in Figure 1. In this case, the effect of transmitted light behind the cell structure is considered negligible. Under this assumption, all the incident photons are finally absorbed inside Si or lost in the following three ways: reflection at the front surface, absorption at the rear Al-BSR, and escape from the cell without absorption. A sum of the above mentioned three losses provide the optical loss of the cell structure. Note that our calculations throughout this paper are on the basis of the properties of steady state solutions, and therefore, the effect of multiple internal reflections inside the cell model was taken into account.

Figure 10 shows the w dependence of the optical loss of a Si cell structure with a 2D submicron grating on the front surface and an Al-BSR on the flat rear surface. In this figure, the values of Λ and d are fixed to $0{\cdot}1$ and $0{\cdot}4\,\mu m$, respectively. These loss spectra show the percentage of non-absorbed photons inside the Si cells. The optical loss near the bandgap wavelength increases with a decrease in w because of the imperfect light trapping of the cell structure.

The spectral optical loss of Si cell structures with different values of Λ and d was calculated in the same manner as that shown in Figure 10. With those results, the total optical loss of the cell structures for the standard solar spectrum was evaluated by the following equation:

$$\text{Loss} = \frac{\int_{0{\cdot}3\,\mu m}^{1{\cdot}12\,\mu m} (1 - \text{Abs}(\lambda)) N_{\text{photon}}(\lambda) d\lambda}{\int_{0{\cdot}3\,\mu m}^{1{\cdot}12\,\mu m} N_{\text{photon}}(\lambda) d\lambda} \tag{5}$$

DOI: 10.1002/pip

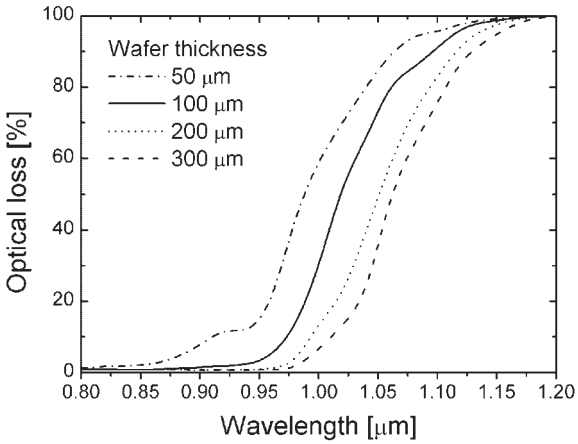

Figure 10. Calculated optical loss spectra of c-Si cell models with a surface texture and rear Al-BSF for several substrate thicknesses w. The surface texture is the 2D pyramid grating with $\Lambda = 0{\cdot}1\ \mu\text{m}$ and $d/\Lambda = 4{\cdot}0$

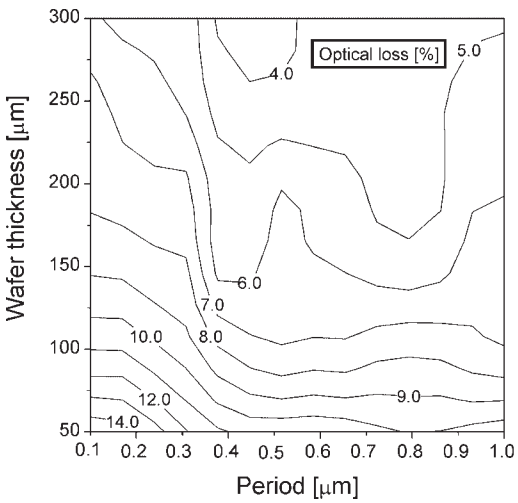

Figure 11. Calculated total optical loss of c-Si cell model with a surface texture and rear Al-BSF as functions of w and Λ. For each Λ, d/Λ was set to the value providing the lowest R_{solar} value according to Figure 4

where Abs is the ratio of the photons absorbed by the Si part of the cell model to the total incident photons. Figure 11 shows the optical loss of the Si cells with submicron-textured surfaces as a function of the wafer thickness, w. For each value of Λ, d/Λ was set such that the lowest value of R_{solar} was obtained, according to Figure 4. As expected, the larger the value of w, the smaller is the optical loss. Surface gratings with smaller values of Λ yield higher optical losses than those with larger values of Λ for the same value of w, whereas all the textures considered here provided low values of R_{solar} of below 3%, as shown in Figure 4. This tendency is particularly observed for thinner substrates having thicknesses of less than 100 μm. This significant loss is attributed to the short optical path length, which is caused by the amount of higher order diffractions being less, as shown in Figure 9.

CONCLUSIONS

In this study, the antireflection and light trapping effects of submicron surface textures in c-Si solar cells were quantitatively investigated by means of numerical simulations with a simple 2D Si surface grating model, and

DOI: 10.1002/pip

two informative results were obtained. First, surface reflection loss can be effectively reduced by using submicron Si gratings over a wide range of periods (0·1–1·0 μm) and appropriate aspect ratios; however, smaller textures less than 0·2 μm require much higher aspect ratios in order to realize a low reflection loss. Second, higher order diffractions by the submicron textures increase the optical path lengths inside c-Si, and periods larger than 0·5 μm are preferable to obtain this effect at higher wavelengths (0·9–1·1 μm) where light trapping is important. From these results, it can be concluded that the submicron textures are effective for light trapping as well as for antireflection in thin c-Si solar cells if appropriate dimensions are chosen. Textures that are much smaller are not beneficial for light trapping; however, they can substantially reduce the surface reflectivity.

In general, RIE-textured surfaces are not perfect periodic structures and have some randomness. However, the results obtained in this study can be applied to the design of surface textures in c-Si solar cells with good optical properties, provided the solar cells possess dimensions such as a period equal to that of surface gratings.

Acknowledgements

This work was partly supported by a Grant-in-Aid from the Ministry of Education, Science, Sports, and Culture, Japan. A part of the calculated results in this research was obtained by using the supercomputing resources at the Information Synergy Center, Tohoku University.

REFERENCES

1. Campbell P, Green MA. Light trapping properties of pyramidally textured surfaces. *Journal of Applied Physics* 1987; **62**: 243–249.
2. Inomata Y, Fukui K, Shirasawa K. Surface texturing of large area multicrystalline silicon solar cells using reactive ion etching method. *Solar Energy Materials and Solar Cells* 1997; **48**: 237–242.
3. Dekkers HFW, Duerinckx D, Szlufcik J, Nijs J. Silicon surface texturing by reactive ion etching. *Opto-Electronics Review* 2000; **8**: 311–316.
4. Zaidi SH, Ruby DS, Gee JM. Characterization of random reactive ion etched-textured Si solar cells. *IEEE Transactions on Electron Devices* 2001; **48**: 1200–1206.
5. Macdonald DH, Cuevas A, Kerr MJ, Samundett C, Ruby D, Widerbaum S, Leo A. Texturing industrial multicrystalline silicon solar cells. *Solar Energy* 2004; **76**: 277–283. DOI: 10.1016/j.solener. 2003.08.019
6. Smith AW, Rohatgi A. Ray tracing analysis of the inverted pyramid texturing geometry for high efficiency silicon solar cells. *Solar Energy Materials and Solar Cells* 1993; **29**: 37–49.
7. Brendel R. Coupling of light into mechanically textured silicon solar-cells—a ray-tracing study. *Progress in Photovoltaics* 1995; **3**: 25–38.
8. Abouelsaood AA, El-Naggar SA, Ghannam MY. Shape and size dependence of the anti-reflective and light-trapping action of periodic grooves. *Progress in Photovoltaics* 2002; **10**: 513–526. DOI: 10.1002/pip·443
9. Heine C, Morf RH. Submicrometer gratings for solar energy applications. *Applied Optics* 1995; **34**: 2476–2482.
10. Moharam MG. Coupled-wave analysis of two-dimensional dielectric gratings. *Proceedings of the Society of Photo-Optical Instrumentation Engineers,* 1988; **883**: 8–11.
11. Sai H, Homare F, Arafune K, Ohshita Y, Yamaguchi M, Kanamori Y, Yugami H. Antireflective subwavelength structures on crystalline Si fabricated using directly formed anodic porous alumina masks. *Applied Physics Letters* 2006; **88**: 201116-1-3. DOI: 10.1063/2205173
12. Asnes DE. Optical properties of Si. In *Properties of Crystalline Silicon*, Hull R (ed.). INSPEC: London & New York, 1999; 683–690.
13. Smith DY, Shiles E, Inokuti M. The optical properties of metallic aluminum. In *Optical Constants of Solids*, Palik ED (ed.). Academic Press: San Diego, 1985; 369–406.
14. Turunen J, Wyrowski F. Diffraction gratings. In *Diffractive Optics for Industrial and Commercial Applications*, Turunen J, Wyrowski F (eds). Akademie Verlag: Berlin, 1997; 7–15.